Supporting Information

A Stretchable Strain-insensitive Temperature Sensor Based on Free-standing Elastomeric Composite Fiber for On-body Monitoring of Skin Temperature

Tran Quang Trung[†±], Thi My Linh Dang[†ǁ], Subramaniyan Ramasundaram,[‡□] Phan Tan Toi,[±] Sang Yoon Park[ǁ*], and Nae-Eung Lee[±Δ⊥*]

[±]School of Advanced Materials Sciences and Engineering, Sungkyunkwan University, Suwon, Kyunggi-do 16419, Korea

[Δ]SKKU Advanced Institute of Nanotechnology, Sungkyunkwan University, Suwon, Kyunggi-do 16419, Korea

[⊥]Samsung Advanced Institute for Health Sciences & Technology, Sungkyunkwan University, Suwon, Kyunggi-do 16419, Korea

[ǁ]Advanced Institutes of Convergence Technology, Seoul National University, Suwon, Kyunggi-do 16229, Korea

[‡] Center for Sustainable Energy Science and Technology, Karunya Institute of Technology and Sciences (KITS), Coimbatore - 641 114, Tamilnadu, India

[□] Department of Chemistry, Karunya Institute of Technology and Sciences (KITS), Coimbatore - 641 114, Tamilnadu, India

[†] These authors contributed equally to this work

E-mail: nelee@skku.edu, yoonpark77@snu.ac.kr

Supporting Figure S1

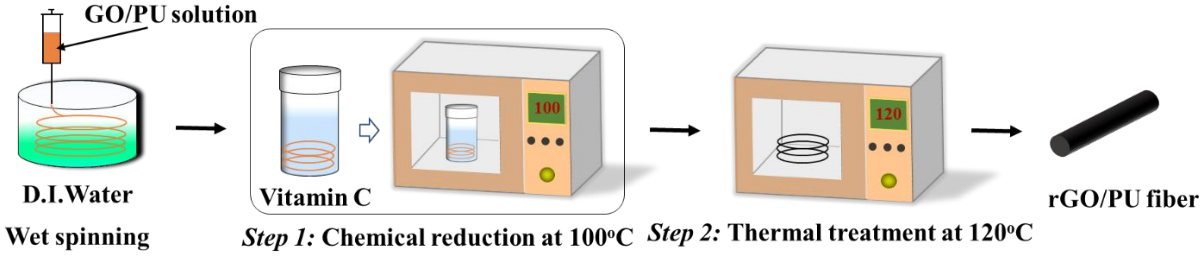

Figure S1: Schematic illustration of the fabrication process of the rGO/PU fiber

Supporting Figure S2

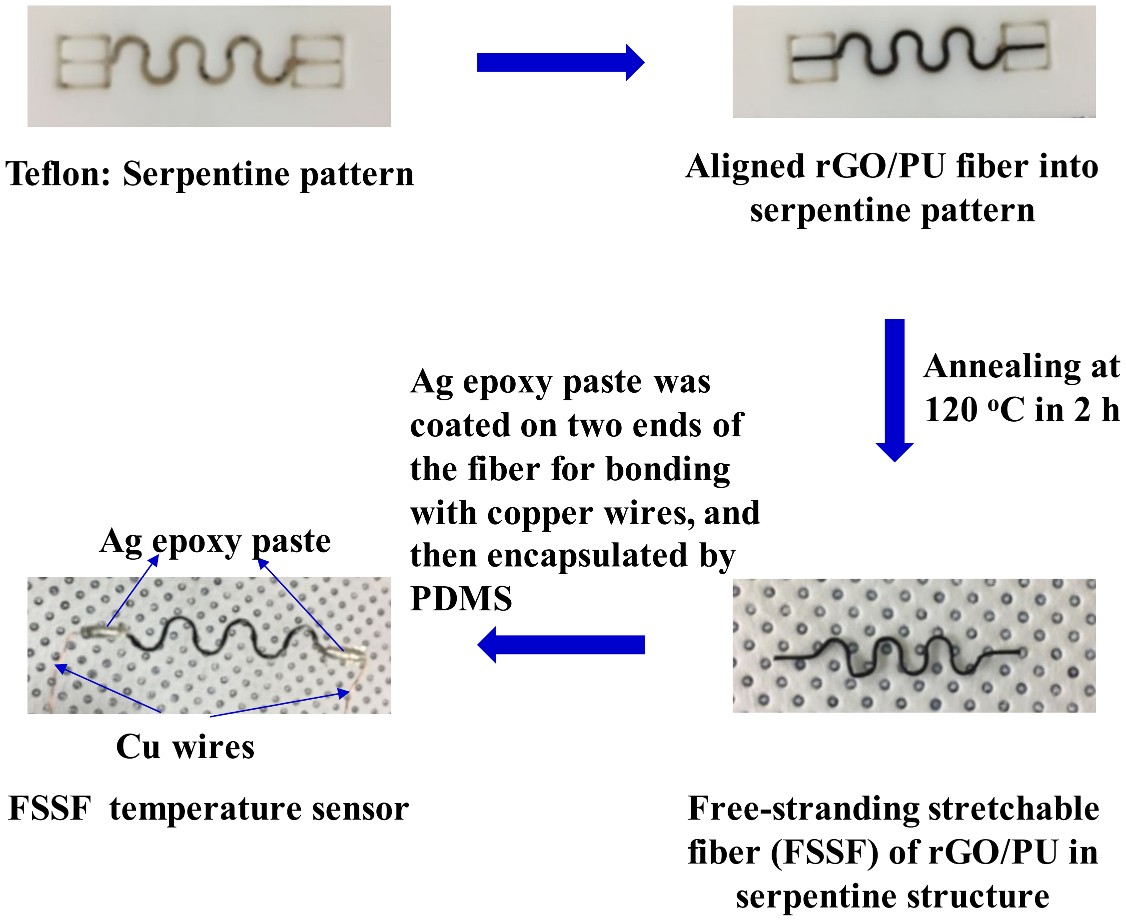

Figure S2: Optical images showing the sequential fabrication process of FSSF temperature sensor

Supporting Figure S3

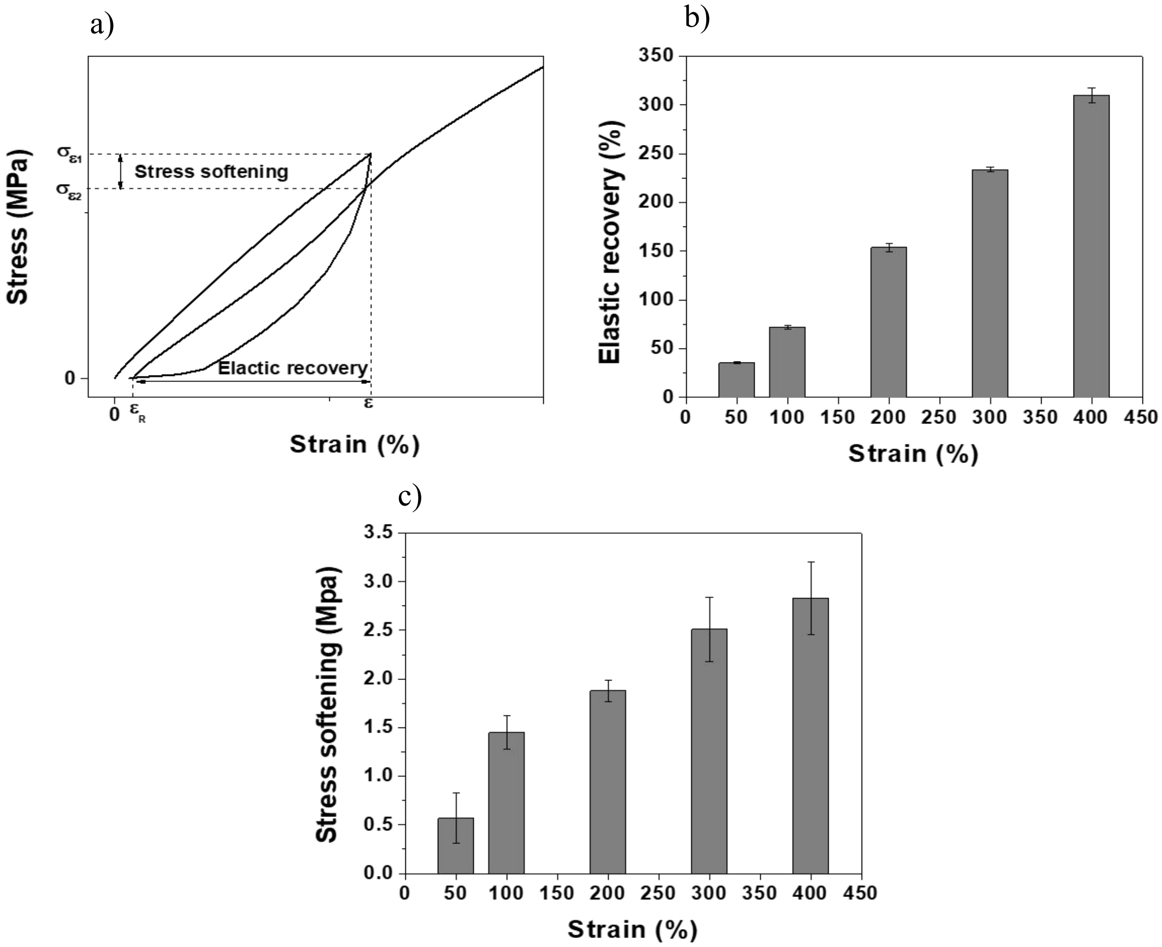

Figure S3: (a) Representation of mechanism based on which the relevant properties, such as elastic recovery and stress softening, are derived from. (b) Loss in elastic recovery of FSSF at various applied strains. (c) Stress softening of FSSF at various applied strains.

Supporting Figure S4

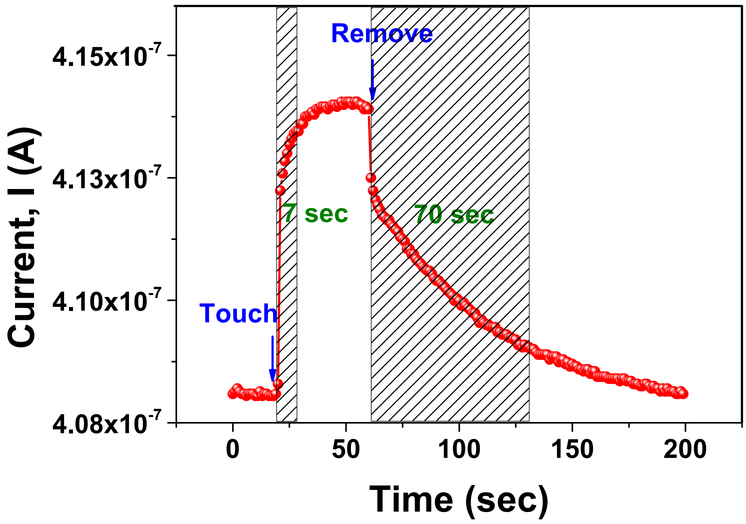

Figure S4: Time-dependent response current of a fabricated device touched with a human finger and extracted values of response time (7 s) and recovery time (70 s).

To evaluate the response and recovery time of the FSSF temperature sensor, a human finger was used as a constant thermal source during touching the FSSF and removing from the FSSF. And, response current of the FSSF with a reduction time of 2 hrs to skin temperature of human finger can be used to calculate the response time and recovery time of the sensor. The results in **Supporting Figure S4** exhibited that the current FSSF increased immediately under finger touch and decrease gradually after removing the finger. From these results, we calculated the response time of the sensor was 7 s (the time required to change from the baseline current to 90% of the peak response current), and the recovery time was 70 s (the time required to move from the peak response current to 90% of the baseline current). Moreover, the response current of the sensor became stable at skin temperature after 15 s upon touching (Supporting Figure S4).

Supporting Figure S5

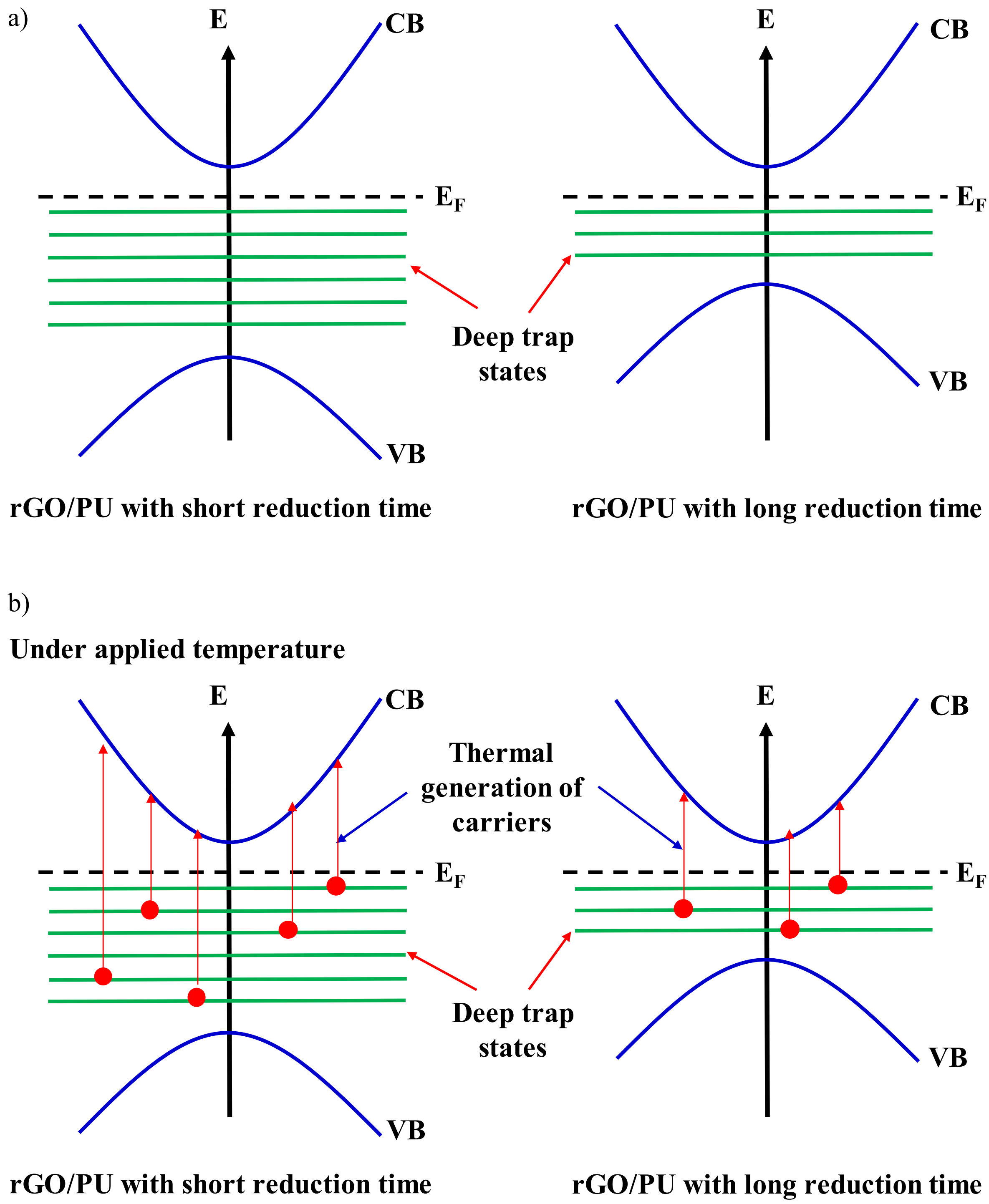

Figure S5: (a) Energy-band structure of the rGO/PU fiber with short- and long-reduction times. (b) Energy-band structure and thermal generation of charge carriers in the rGO/PU fibers with short- and long-reduction times.

Supporting Figure S6

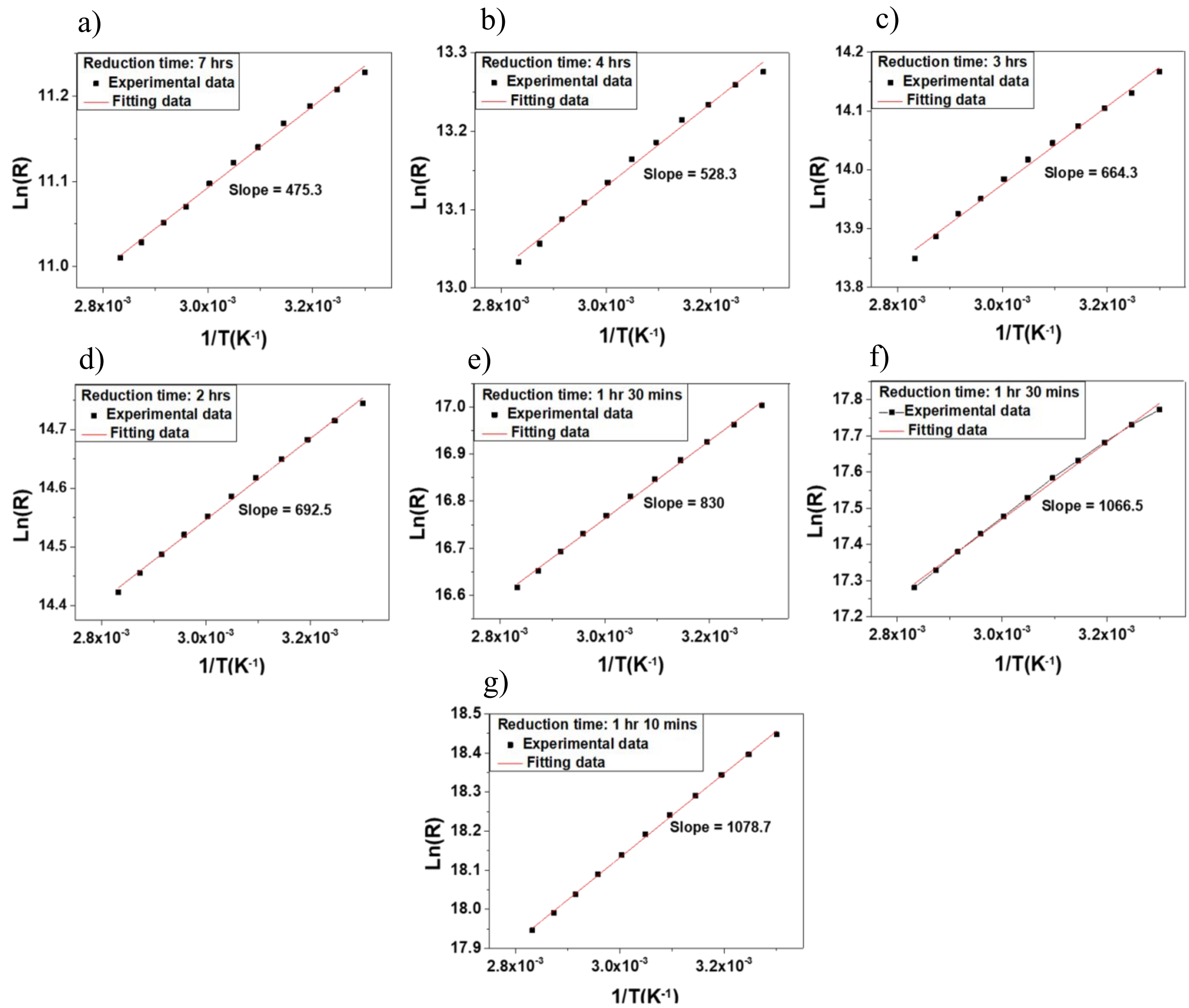

Figure S6: Plot of ln(R) versus 1/T for FSSFs with GO reduction times of 7 hrs (a), 4 hrs (b), 3 hrs (c), 2 hrs (d), 1 hr 30 mins (e), 1 hr 20 mins (f), and 1 hr 10 mins (g).

Supporting Figure S7

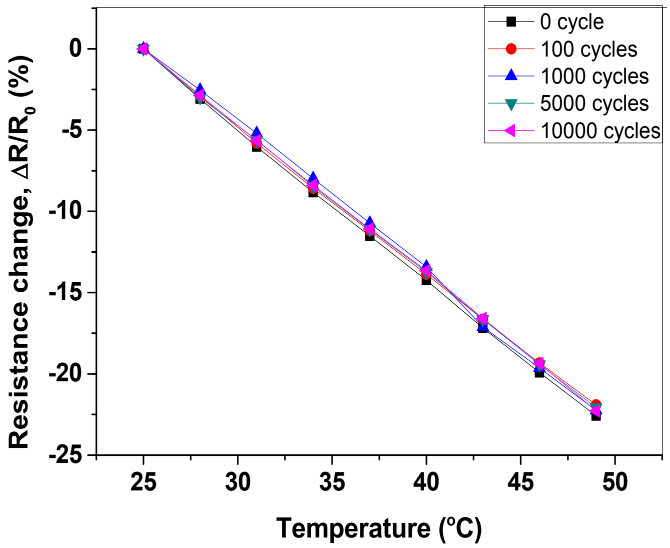

Figure S7: Responsivity of the FSSF temperature sensor with a GO reduction time of 1 hr 20 mins for applied cyclic stretching using 0, 100, 1000, 5000, and 10000 cycles at a strain of 50 %.

Supporting Figure S8

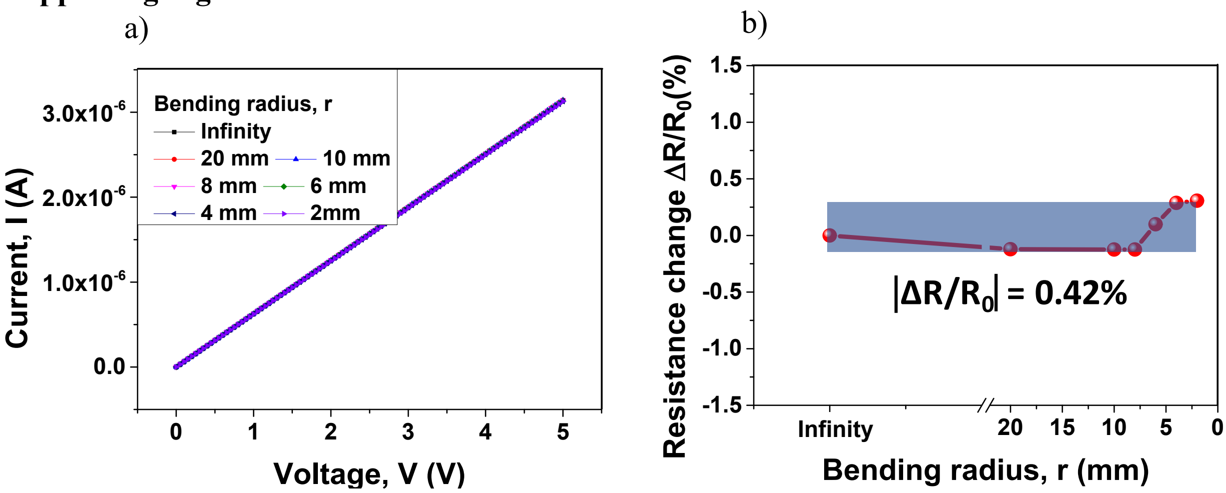

Figure S8: (a) I-V curves of the FSSF temperature sensor on PDMS substrate under bending radius of 20, 10, 8, 6, 4, 2 mm. (b) Resistance change of the FSSF temperature sensor on PDMS substrate as function of bending radius.

To evaluate the effect of bending on the resistance of the FSSF temperature sensor, the I-V curves of the sensor under applied various bending radius (20, 10, 8, 6, 4, and 2 mm) were measured and presented in **Supporting Figure S8a**. Based on these results, the $\frac{\Delta R}{R_0}$ values of the sensor under bending radius of 20, 10, 8 ,6 ,4, 2 mm were also calculated and presented in **Supporting Figure S8b**. These results demonstrated that the absolute $\frac{\Delta R}{R_0}$ owing to the effect of bending is 0.42 %, which corresponds to ± 0.45 °C of inaccuracy in the temperature reading. This means that the FSSF temperature sensor on PDMS is fairly free from straining signal interference due to bending.

Supporting Figure S9

a)

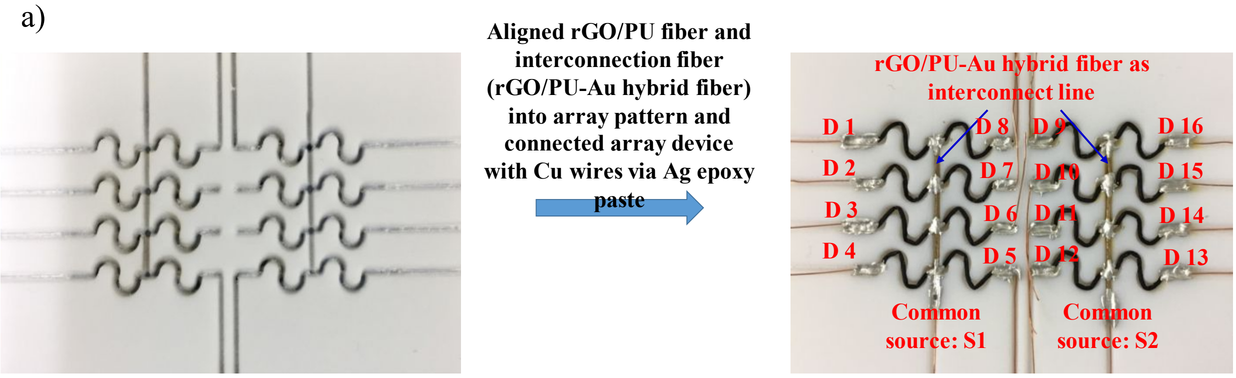

Teflon: Serpentine pattern in 4x4 array

FSSF temperature sensor in array structure

b)

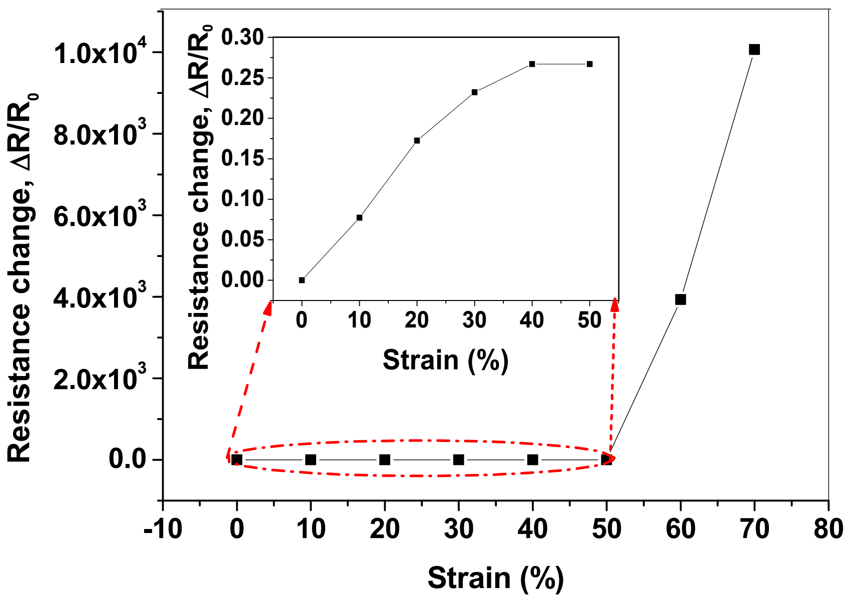

Figure S9: (a) Optical images showing the fabrication process of the FSSF temperature sensor in a 4×4 array structure. (b) Resistance change ($\Delta R/R_0$) of the rGO/PU–Au fiber during stretching. The inset presented the enlarged figure of the resistance change of the fiber under strain of 0 to 50 %.

The FSSF temperature sensor in a 4×4 array was fabricated based on two common electrodes S1 and S2, and based on sixteen electrodes D1 to D16. These common sources and drains were connected with Cu wires via Ag epoxy paste. For the interconnection of the devices in the array we developed a stretchable conductive rGO/PU–Au fiber which was fabricated using a stretch-release method. An rGO/PU fiber with a diameter of 550 µm and a GO reduction time of 1 h 20 min was prestretched up to 100 % followed by the deposition of an Au layer on it with a thickness of 60 nm using thermal evaporation. Subsequently, the Au-coated rGO/PU fiber was released to generate a stretchable interconnected fiber. The electrical properties of the rGO/PU–Au fiber under stretching is studied and presented in **Figure S9b**. The results demonstrate that the rGO/PU–Au fiber can be stretched up to 50 % with a very small resistance changes (see inset figure in **Figure S9b**). If the fiber is stretched up to over 50 %, the resistance of the fiber will be sharply increased. This was contributed by the recovery characteristics of the rGO/PU fiber coated with Au which was not completely recovered to initial state. Due to thermal expansion of the fiber during deposition of Au layer thermal evaporation, the Au-coated rGO/PU fiber has just recovered around 50 % of its initial state.

Supporting Figure S10:

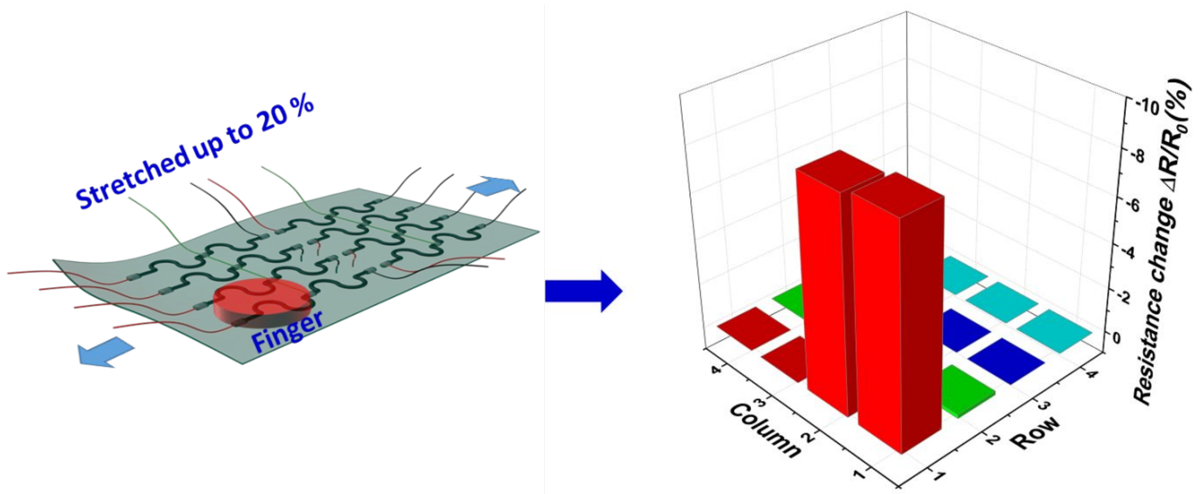

Figure S10: Distribution of $\Delta R/R_0$ values when a finger touches two devices of the device array under strain of 20 %.